Polym. Bull. (2016) 73:2677–2688
DOI 10.1007/s00289-016-1614-6

ORIGINAL PAPER

Characterization of nanocomposite laminates fabricated from aqueous dispersion of polyvinylpyrrolidone and L-leucine amino acid modified-montmorillonite

Shadpour Mallakpour[1,2,3] · Marziyeh Khani[1]

Received: 30 June 2015 / Revised: 5 January 2016 / Accepted: 26 January 2016 /
Published online: 5 February 2016

Abstract This study presents a favorable, simple, safe, fast, and facile approach for the synthesis of potentially ecofriendly biodegradable polymer nanocomposites (NC)s with amino acid modified-montmorillonite (AA-MMT). At first, positively charged chiral amino acid L-leucine was incorporated into the unmodified Cloisite-Na^+ montmorillonite (MMT) for organo-modification of MMT by cation-exchange method. Fourier transform infrared spectroscopy (FT-IR) showed the presence of the organic segment in the modified clay product. Then the dispersion characteristics of AA-MMT in the aforementioned NCs were determined based on polyvinylpyrrolidone (PVP). The obtained NCs were characterized by different analytical tools including FT-IR, powder X-ray diffraction (XRD), thermogravimetric analysis (TGA), transmission electron microscopy (TEM), and field emission scanning electron microscopy (FE-SEM). The XRD patterns, FE-SEM, and TEM results proposed that the AA-MMT platelets were intercalated with PVP during the process. As evidenced by TGA analysis of the obtained NCs, heat stability was slightly improved as compared with the pure PVP.

Keywords Amino acid modified-montmorillonite · Polymer–clay nanocomposites · Solution intercalation process · Polyvinylpyrrolidone · Morphology study

✉ Shadpour Mallakpour
mallakpour84@alumni.ufl.edu; mallak@cc.iut.ac.ir; mallak777@yahoo.com

[1] Organic Polymer Chemistry Research Laboratory, Department of Chemistry, Isfahan University of Technology, Isfahan 84156-83111, Islamic Republic of Iran

[2] Nanotechnology and Advanced Materials Institute, Isfahan University of Technology, Isfahan 84156-83111, Islamic Republic of Iran

[3] Department of Chemistry, Center of Excellence in Sensors and Green Chemistry, Isfahan University of Technology, Isfahan 84156-83111, Islamic Republic of Iran

Introduction

Over the past decade, in the area of research and development, an enormous amount of attention has been paid to the polymer nanocomposites (PNC)s [1]. While conventional inorganic fillers are typically added in percentages varying from 20 to 40 % by weight, in PNCs, the usual amount could be between 2 and 5 % [2, 3]. Among the nanoparticulates, carbon nanotubes and layered silicate (LS)s have been extensively investigated. More specifically, LSs are favored in commercial applications over carbon nanotubes because of their low-cost and abundance [4, 5]. Many works have revealed that the addition of a very low percentage of LSs can bring about an important improvement in numerous properties, for instance, flame retardancy, gas barrier properties, stiffness and strength, thermal stability, ionic conductivity, electrical properties, and biodegradability [6–8]. All of these properties make these materials suitable for a wide range of applications, such as food packaging, automotive industry, electronics, biomedicine, and biotechnology [9–11].

Among the layered nanofillers, MMT clay is one of the most extensively used nanofillers for the synthesis of PNCs, owing to its high ion-exchange capacity for the attachment of surfactant molecules, and high aspect ratio for improved barrier properties [12]. Moreover, MMT is made of numerous stacked silicate layers with a regular gap or gallery in each one [13, 14]. The MMT clay contains planar layers of octahedral (O) bounded by tetrahedral (T) over and below with a typical repeat distance (gallery spacing) between the T–O–T layers [9, 15, 16].

The organic compound can be either intercalated or exfoliated with the inorganic filler. Intercalation happens when a small quantity of macromolecule goes into the gallery spacing and separates the layers somewhat, but fails to separate the layers entirely. Exfoliation (or delamination) occurs when the clay platelets are pushed apart and dispersed homogenously into the macromolecule matrix [16].

The affinity of the macromolecule to the surface of the clay, and/or to the organic surfactant of the organoclay is crucial for further acceptable interactions among these segments which can increase high levels of exfoliation [17, 18]. The surface treatment of clay has received great attentions, for instance, ion exchange of the inorganic cations with organic cations typically with quaternary ammonium compounds can intensely change the surface properties. The intercalation of a cationic surfactant not only changes the surface properties from hydrophilic to hydrophobic but also importantly increases the d-spacing of the layers [19, 20].

There is a growing interest in improving novel macromolecule clay NCs to meet the new demands in all the fields. As the polyvinylpyrrolidone (PVP) is widely utilized as an adhesive in textile dye stripping, an industrial surfactant, an extender in pharmaceutical applications, and an emulsifier, it is good to examine PVP/organo-clay NCs which may display good thermal stability and other properties [21–23]. In the case of NCs based on PVP, mixing in water solution is one of the most frequently recounted approaches. This is because PVP is dissolved well in water as well as in many common polar solvents [22]. Many clay mineralogists have considered the structure of the clay NC consisting of PVP because of its specific interactions with clay minerals. The

strong absorption of this macromolecule on the clay surface was witnessed, however, the mechanism is still not well unstated [24–26].

Yet, there were some articles on PVP/MMT, and PVP/organomodified MMT NCs [21–23, 26]. But in these papers, they did not utilize optically active and biodegradable amino acid coupling agent for the preparation of amino acid modified-montmorillonite (AA-MMT). This research work was carried out with a view to prepare potentially biodegradable NCs consisting of bioactive polymer and chiral nanoclay. Dispersion of this chiral nanoclay into PVP matrix was expected to increase its thermal and physical properties and also make them more biodegradable and biocompatible. When compared with chemically synthesized surfactant, amino acid biosurfactants have the important advantage of biodegradability, low toxicity, low-cost and various possible structures [27–29].

Actually, in the present investigation, PVP/AA-MMT NCs with different percentages of AA-MMT (3, 5, and 7 wt%) were prepared by a green and environmentally friendly process and characterized. The data analysis revealed that the aforementioned NCs showed slightly improved thermal stability.

Experimental

Materials

The silicate used, Cloisite-Na^+, was purchased from Southern Clay Products, Gonzales, Texas (USA). The cation-exchange capacity (CEC) of Cloisite-Na^+ is 92.6 meq/100 g as reported by suppliers. This compound was used without any further purification. Other reagents and solvent were provided commercially from Aldrich Chemical Co. (Milwaukee, WI), Fluka Chemical Co. (Buchs, Switzerland) and Merck Chemical Co. (Darmstadt, Germany) and were used as received. The PVP MW = 40,000 received from Merck Chemical Co.

Equipments

Fourier transform infrared (FT-IR) spectra data were taken on Jasco-680 spectrophotometer (Japan) at a resolution of 4 cm^{-1} and they were scanned at wavenumber range of 400–4000 cm^{-1}. Vibration bands were described as wave number. FT-IR spectra of solid sample were also attained by building their pellets in KBr. Blank scanning was executed before measurements to remove the effect of water vapor and CO_2 in the air. The data of thermal gravimetric analysis (TGA) was done using STA503 TA instrument (Hüllhorst, Germany) in a nitrogen atmosphere at a heating rate of 20 °C/min. X-ray diffraction pattern were taken on a Bruker, D8 ADVANCE, (Karlsruhe, Germany) diffractometer operating at the current of 40 mA and a voltage of 45 kV. The Cu Kα radiation source ($\lambda = 1.5418$ Å) was used in the range of 0.8°–10° at a scanning rate of 0.02°/s. XRD information was acquired from samples powdered and measured for 2θ. Field emission scanning electron microscopy (FE-SEM) micrographs were collected on HITACHI (S-4160)

(Tokyo, Japan). To clarify the nanostructure of the samples, TEM (CM 120, Philips) was also used at an accelerating voltage of 100 kV. For TEM, NCs were suspended in water and a small drop of suspension was deposited on the carbon coated copper grid. The construction of the aforementioned NCs was performed on a MISONIX ultrasonic liquid processor, XL-2000 SERIES. Sonication was carried out with the probe of the ultrasonic horn being absorbed directly in the mixture solution system with a frequency of 2.25×10^4 Hz and power of 100 W.

Preparation of organomodified Cloisite-Na^+

According to our previous work, L-leucine was utilized for the modification of MMT clay by cation-exchange method [30].

Construction of PVP/AA-MMT NCs

For the 3, 5, and 7 wt% AA-MMT concentration (weight fraction concentration for 1 g of polymer matrix) 0.03, 0.05 and 0.07 g of organomodified MMT powder was dispersed in deionized water and stirred vigorously for 2 h. Afterwards, it was sonicated for 30 min. Then 1 g of PVP was added to AA-MMT solution and stirred for an additional period of 30 min to attain a homogeneous mixture. Finally, this solution was casted into polystyrene-Petri-dishes. Bubbles were removed by shaking. The cast Petri-dishes were kept at R.T. until they were dried and then dried at 60 °C under vacuum for 2 h.

Results and discussion

Production of NCs

This chemical modification alters the nature of MMT from a purely inorganic to an organic-like matter, or it forms a hydrophilic to a hydrophobic substance. This intercalation increases the spacing between the MMT layers and even leads to the complete exfoliation of the layers to form MMT/polymer NCs. Organoclay has electronegative oxygen and hydroxyl groups, which can assist the adsorption of PVP onto its surface. After the preparation of organo-modified-MMT, PVP/AA-MMT NCs were successfully fabricated by adding various AA-MMT contents (3, 5, and 7 wt%) to the PVP via solution intercalation method (Scheme 1).

FT-IR study of NCs

The FT-IR spectroscopy was used to characterize the chemical structure of organo-modified-MMT and NCs, and the obtained spectra are shown in Fig. 1. The FT-IR spectra of AA-MMT (Fig. 1a) showed the characteristic absorptions at 3635, 3423 and 1703 cm^{-1}, corresponding to –OH stretching of Al–OH and Si–OH, –NH and C=O groups, respectively. The characteristic band observed at 2926 cm^{-1} was due to C–H stretching vibration of CH_2 aliphatic for L-leucine moiety. Also this

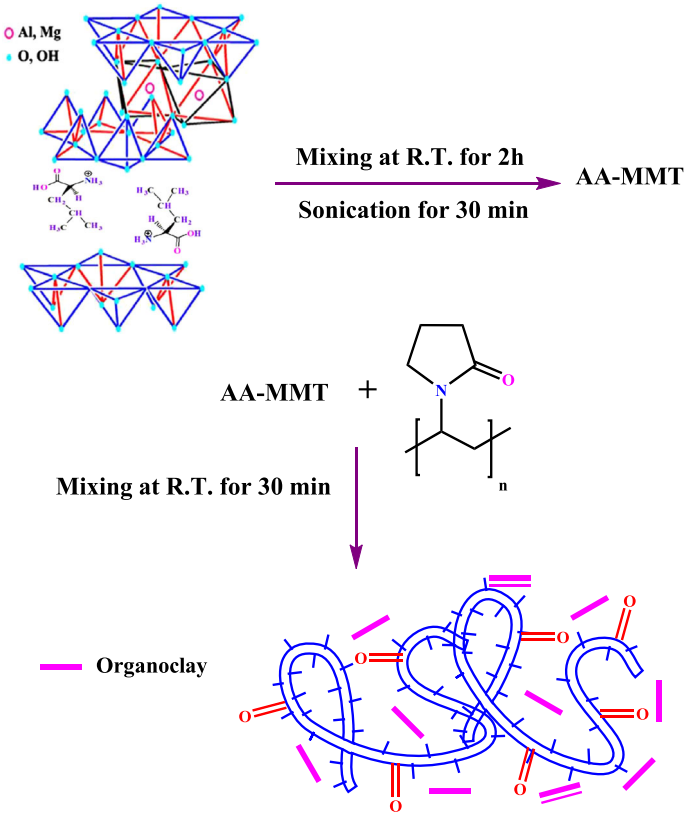

Scheme 1 Schematic image of the fabrication of PVP/AA-MMT NCs

spectrum displayed bands in the 400–600 cm^{-1} area that were related to Mg–O and Al–O bending vibration. The typical characteristic stretching hydroxyl band of L-leucine was shown at 2500–3500 cm^{-1} [30]. As the AA-MMT was loaded into the PVP, the clay band intensity became stronger in the FT-IR spectra (Fig. 1c–e) [11]. The peak at 1663 cm^{-1} was related to carbonyl of PVP. In the spectra of NCs, the characteristic absorption bands of the AA-MMT and PVP were observed. Consequently, the functional groups of the obtained PVP/AA-MMT NCs were confirmed by the data of FT-IR spectra.

X-ray diffraction data

According to XRD patterns of the MMT and AA-MMT, the basal spacing of the unmodified MMT was clearly increased from 1.17 to 1.47 nm for an MMT modified with L-leucine amino acid [30]. The d-spacing of the clay and AA-MMT was analyzed by using Bragg's equation ($n\lambda = 2d \sin \theta$, $\lambda = 1.5418$ Å). The aforementioned PVP/AA-MMT NCs were presumably classified into two types, intercalated and exfoliated NCs. The structure of PVP/AA-MMT NCs could be

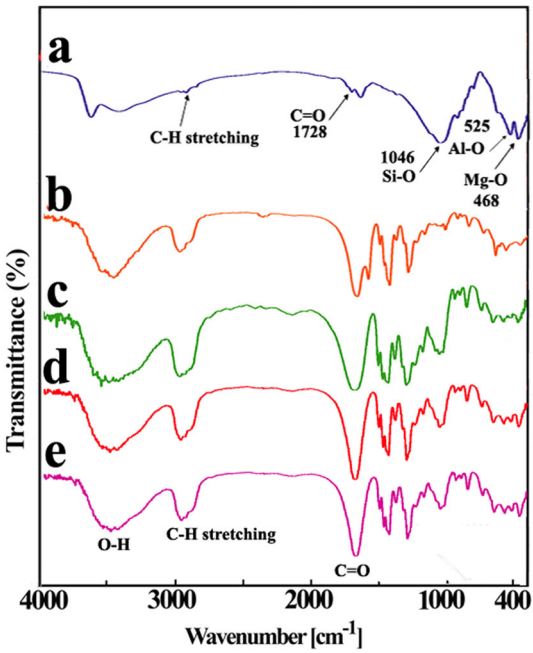

Fig. 1 FT-IR spectra of *a* AA-MMT, *b* PVP, *c* PVP/AA-MMT NC (3 wt%), *d* PVP/AA-MMT NC (5 wt%), and *e* PVP/AA-MMT NC (7 wt%)

recognized by determining the shape, position, and intensity of basal reflections in clay layers. The specific peak of clay would seem to be in a lower degree on XRD pattern due to the increase of the distance between the layers. But in the exfoliated type, the peak of silicate layer would disappear because the layered structures between clay were interrupted by intercalated macromolecules [31, 32]. According to the obtained results, the morphology of PVP/AA-MMT NCs was intercalated. Consistent with Fig. 2c (PVP/AA-MMT NC 3 wt%), the characteristic peak of AA-MMT with the layer distance equal to 1.47 nm moved to 4.82 nm with the broadening peak. It could be attributed to the intercalation of PVP matrix into the clay gallery and the partial disturbance of stacked layer parallel to each AA-MMT. In Fig. 2d (PVP/AA-MMT NC 7 wt%) two peaks at different interlayer spaces are reported which can be a symptom of the presence of different *d*-spacing. The presence of the second-order peak characteristically offers that a high degree of periodic order is current in the material [33]. On the other hand, it could be related to a two orders of (00 *l*) Bragg diffraction peaks of clay crystals appear in PVP NCs.

Morphology

FE-SEM

FE-SEM analysis highlighted the homogeneity of the pristine PVP and NCs (Fig. 3). According to our previous work, pristine PVP exhibited a dense and homogeneous morphology [34]. The clay layers (white small scenting layers) in

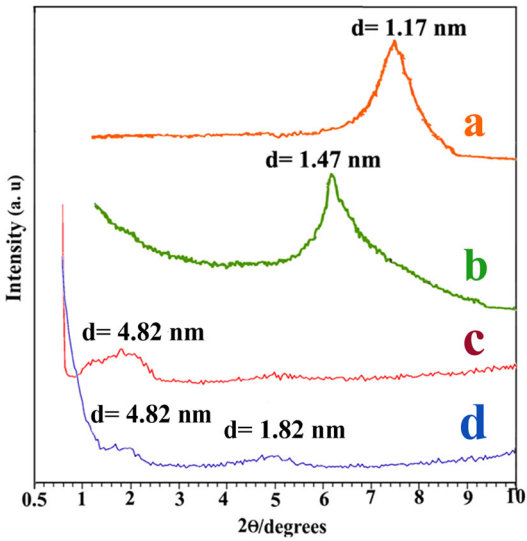

Fig. 2 XRD curves of *a* MMT, *b* AA-MMT, *c* PVP/AA-MMT NC (3 wt%), and *d* PVP/AA-MMT NC (7 wt%)

PVP/AA-MMT NCs could be seen in its surface at FE-SEM micrograph (Fig. 3a–f). By comparison of the morphologies of PVP [34] and PVP/AA-MMT NCs, it is apparent that the morphology of the PVP in the aforementioned NCs was changed to nanospherical shape. The FE-SEM observations showed the compatibility between PVP and AA-MMT and also, the homogeneity of the above NCs. The morphology of the NCs was affected by the presence of organo-modified clay due to the change in the arrangements of ions in the modified NCs. Meanwhile, the organo-modified-MMT contained hetero-atoms functional groups such as: –NH and –OH segment, which could be expected to have more favorable interactions between AA-MMT and the PVP chains. As the AA-MMT content was increased, the agglomeration didn't occur at various percentages of clay loading, which might be due to the modification of layers with amino acid moiety. Inappropriately, it is difficult to find regularly intercalated nanostructured NC as indicated by the XRD patterns at this magnitude. In some places, there are some curved layers for AA-MMT.

TEM results

To find whether the AA-MMT were exfoliated or not in the NCs, TEM images were used to investigate the morphology of the PVP/AA-MMT NC 5 wt% with magnifications of 250 and 300 nm (Fig. 4). The ultrasonic energy was applied to the NCs before TEM imaging, causing the homogenous dispersion of NCs for micrograph. The black lines in the TEM micrographs characterize the AA-MMT platelets while the gray background corresponds to PVP matrix. Figure 4 illustrates that the polymer has entered into the intergallery spacing where the layer structure of clay was moderately being disrupted. Also this figure supports that the organoclay is dispersed randomly in the polymer matrix in a nanometer scale. Therefore, the above results clearly demonstrated the good dispersity of the AA-

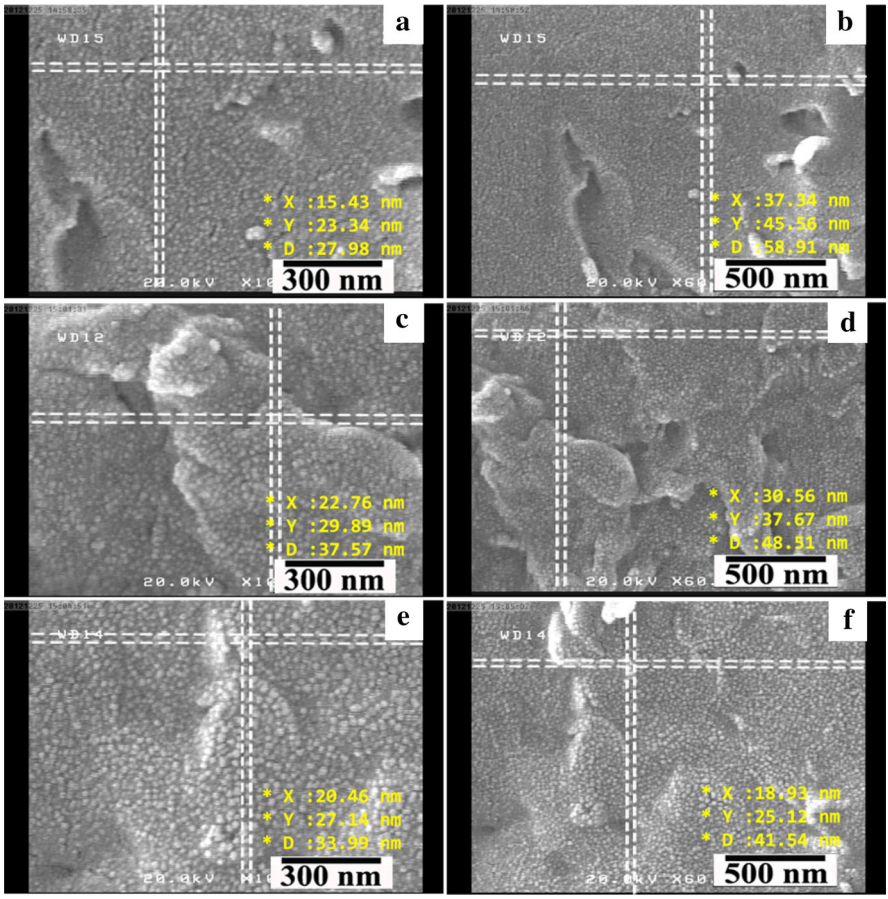

Fig. 3 FE-SEM micrographs of **a**, **b** PVP/AA-MMT (3 wt%), **c**, **d** PVP/AA-MMT NC (5 wt%), and **e**, **f** PVP/AA-MMT NC (7 wt%) with different magnifications

MMT and the virtually disorganized distribution in the NCs, which agrees with the XRD results shown in Fig. 2. This could be attributed to the amino acid modifier for modification of MMT. It is implied that diffusion of polymer chains inside clay galleries is less hindered due to increased d-spacing. Thus, the structure of organic modifier within organoclay is an important factor to affect the morphology of the aforementioned NCs.

TGA analysis

Thermal stability is typically investigated by TGA. Heat stability is a significant property for the NCs containing MMT. In this planning, TGA was performed under nitrogen purge flow to avoid the oxidation of the aforementioned NCs (Fig. 5). The temperature corresponding to 5 % (T_5) and 10 % (T_{10}) of weight loss, char yield at 800 °C and also, the limiting oxygen index (LOI) obtained from TGA curve have

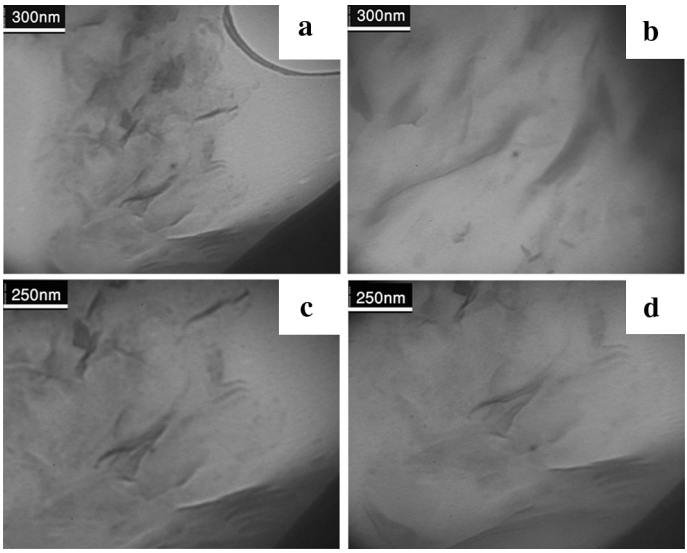

Fig. 4 TEM micrographs of PVP/AA-MMT NC (5 wt%) with different magnifications

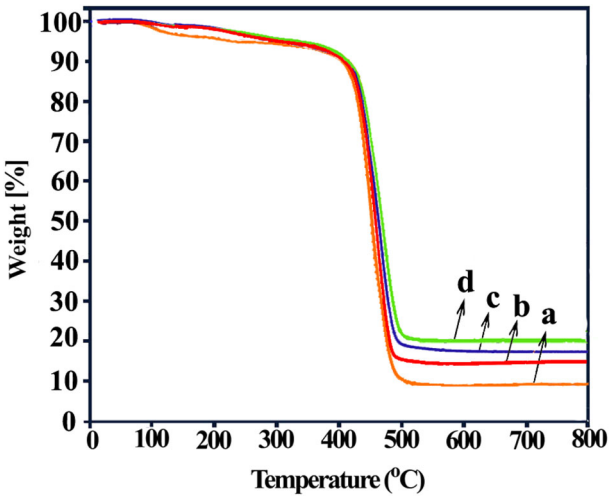

Fig. 5 TGA thermograms of *a* PVP, *b* PVP/AA-MMT NC (3 wt%), *c* PVP/AA-MMT NC (5 wt%) and *d* PVP/AA-MMT NC (7 wt%) under nitrogen atmosphere at the heating rate of 20 °C/min

been brought in Table 1. Limiting oxygen index (LOI) of the macromolecules can be calculated from Char yield quantity based on Van Krevelen and Hoftyzer equation [35].

$$\mathrm{LOI} = 17.5 + 0.4\mathrm{CR}$$

where CR = char yield.

Table 1 Thermal properties of the PVP and PVP/AA-MMT NCs

Sample	T_5 (°C)[a]	T_{10} (°C)[b]	Char yield (%)[c]	LOI[d]
PVP	227	403	9	21.3
PVP/AA-MMT NC (3 wt%)	303	405	15	23.5
PVP/AA-MMT NC (5 wt%)	335	407	17	24.3
PVP/AA-MMT NC (7 wt%)	347	415	20	25.5

[a] Temperature at which 5 % weight loss was recorded by TGA at heating rate of 20 °C//min under a nitrogen atmosphere

[b] Temperature at which 10 % weight loss was recorded by TGA at heating rate of 20 °C//min under a nitrogen atmosphere

[c] Weight percentage of material left undecomposed after TGA analysis at a temperature of 800 °C under a nitrogen atmosphere

[d] Limiting oxygen index (LOI) evaluating char yield at 800 °C

According to Fig. 5, the initial weight loss of the NCs was not remarkably changed, but after the temperature of around 460 °C, the heat stability of the resulting NCs rose with the increasing percentage of AA-MMT in the macromolecule matrix due to the high cation exchange capacity, prominent thermal stability of clay and compatibility of the organomodified-MMT with PVP [21, 34]. Table 1 indicates that the char yield was increased from 9 % for neat PVP to 20 % for PVP/AA-MMT NC (7 wt%). The char yield of the resulting NCs was increased as the content of AA-MMT was increased, because of the high thermal resistance of clay. Results of TGA of NCs PVP/MMT obtained with Zabska et al. indicate that addition of MMT causes a slight decrease in thermal stability of nanocomposites when compared to neat polymer. The stability increases with increase in clay loading reaching at 20 wt% of the filler nearly the stability level of the polymer [22].

Conclusions

Novel polymer/layered silicate NCs built from PVP and MMT interlayer using L-leucine amino acid as the organo-modifier by solution intercalation method. Chiral AA-MMT was prepared by using ammonium salt of natural L-leucine amino acid and Cloisite-Na^+. The characteristic analysis of the resulting NCs showed that an appropriate interaction happened between the modified MMT and the organic counterpart. TEM and FE-SEM micrograph characterized the good dispersion of organoclay in the PVP matrix and intercalation structure in NCs. From the XRD pattern, the specific peak of clay layers moved to the lower angles with widening and lower intensity, confirming the addition of interlayer spacing of organoclay in the aforementioned NCs and the formation of intercalated NCs. Likewise, the existence of AA-MMT in the polymer matrix was studied by FT-IR. The PVP/AA-MMT NCs also demonstrated somewhat improved heat stability and char yield, as compared with the pure PVP. It was related to the clay that not only acted as a

thermal barrier, but also increased the thermal stability by forming char. PVP and its composites are potentially applied in a variety of industrial application, for example, in pharmacy and medicine, synthetic plasmas as well as hydrogels and thromboresistent hydrophilic gels.

Acknowledgments The authors thank the Research Affairs Division of Isfahan University of Technology (IUT), Isfahan for partial financial support. Further financial support from Iran nanotechnology Initiative Council (INIC), National Elite Foundation (NEF) and Center of Excellence in Sensors and Green Chemistry Research (IUT) is gratefully acknowledged.

References

1. Nevalainen K, Vuorinen J, Villman V, Suihkonen R, Jarvela P, Sundelin J, Lepisto T (2009) Characterization of twin-screw-extruder-compounded polycarbonate nanoclay composites. Polym Eng Sci 49:631–640
2. Ghaffarpour Jahromi S, Khodaii A (2009) Effects of nanoclay on rheological properties of bitumen binder. Constr Build Mater 23:2894–2904
3. Barghamadi M (2010) Kinetics and thermodynamics of isothermal curing reaction of epoxy-4, 4′-diaminoazobenzene reinforced with nanosilica and nanoclay particles. Polym Compos 31(8):1442–1448
4. Aktas L, Altan MC (2010) Characterization of nanocomposite laminates fabricated from aqueous dispersion of nanoclay. Polym Compos 31(4):620–629
5. Ahmadi SJ, Huang YD, Li W (2004) Synthetic routes, properties and future applications of polymer-layered silicate nanocomposites. J Mater Sci 39:1919–1925
6. Grigoriadi K, Giannakas A, Ladavos AK, Barkoula NM (2015) Interplay between processing and performance in chitosan-based clay nanocomposite films. Polym Bull 72(5):1145–1161
7. Amin A, Kandil H, Awad HM, Ismail MN (2015) Preparation and characterization of chitosan–hydroxyapatite–glycopolymer/Cloisite 30 B nanocomposite for biomedical applications. Polym Bull 72(6):1497–1513
8. Abedi S, Abdouss M, Daftari-Besheli M, Ghafelehbashi SM, Azadi F, Nokhbeh SR, Safinejad A (2013) Highly exfoliated PE/Na^+ MMT nanocomposite produced via in situ polymerization by a catalyst supported on a novel modified Na^+ MMT. Polym Bull 70(10):2783–2792
9. Barick AK, Tripathy DK (2010) Effect of organoclay on the morphology, mechanical, thermal, and rheological properties of organophilic montmorillonite nanoclay based thermoplastic polyurethane nanocomposites prepared by melt blending. Polym Eng Sci 50(3):484–498
10. Meng X, Wang H, Qian Z, Gao X, Yi Q, Zhang S, Yang M (2009) Preparation of photodegradable polypropylene/clay composites based on nanoscaled TiO_2 immobilized organoclay. Polym Compos 30(5):543–549
11. Wang YC, Fan SC, Lee KR, Li CL, Huang SH, Tsai HA, Lai JY (2004) Polyamide/SDS–clay hybrid nanocomposite membrane application to water–ethanol mixture pervaporation separation. J Membrane Sci 239:219–226
12. Wang DY, Liu XQ, Wang JS, Wang YZ, Stec AA, Hull TR (2009) Preparation and characterisation of a novel fire retardant PET/a-zirconium phosphate nanocomposite. Polym Degrad Stabil 94:544–549
13. Kandola BK, Smart G, Horrocks AR, Joseph P, Zhang S, Hull TR, Ebdon J, Hunt B, Cook A (2008) Effect of different compatibilisers on nanoclay dispersion, thermal stability, and burning behavior of polypropylene–nanoclay blends. J Appl Polym Sci 108:816–824
14. Moghri M, Akbarian M (2009) Effects of nanoclay and additives on the fusion characteristics and thermal stability of poly(vinyl chloride) nanocompounds. J Vinyl Addit Techn 15(2):92–98
15. Ogawa M, Takizawa Y (1999) Intercalation of alkylammonium cations into a layered titanate in the presence of macrocyclic compounds. Chem Mater 11(1):30–32
16. Chao TY, Chang HL, Su WC, Wu JY, Jeng RJ (2008) Nonlinear optical polyimide/montmorillonite nanocomposites consisting of azobenzene dyes. Dyes Pigments 77:515–524
17. Zhang X, Loo LS (2008) Morphology and mechanical properties of a novel amorphous polyamide/nanoclay nanocomposite. J Polym Sci Part B Polym Phys 46:2605–2617

18. Huang JC, Zhu ZK, Ma XD, Qian XF, Yin J (2001) Preparation and properties of montmorillonite/organo-soluble polyimide hybrid materials prepared by a one-step approach. J Mater Sci 36:871–877
19. Ganguly S, Dana K, Mukhopadhyay TK, Ghatak S (2011) Simultaneous intercalation of two quaternary phosphonium salts into montmorillonite. Clay Clay Miner 59:13–20
20. Xi Y, Frost RL, He H (2007) Modification of the surfaces of Wyoming montmorillonite by the cationic surfactants alkyl trimethyl, dialkyl dimethyl, and trialkyl methyl ammonium bromides. J Colloid Interface Sci 305:150–158
21. Ramesh S, Sivasamy A, Alagar M, Chandrasekar F (2010) Synthesis and characterization of poly(n-vinyl-2-pyrrolidone)-organo-modified montmorillonite (OMMT) clay hybrid nanocomposites. J Compos Mater 45(14):1483–1489
22. Zabska M, Jaskiewicz K, Kiersnowski A, Szustakiewicz K, Rathgeber S, Piglowski J (2011) Spontaneous exfoliation and self-assembly phenomena in polyvinylpyrrolidone/synthetic layered silicate nanocomposites. Radiat Phys Chem 80:1125–1128
23. Dornelas CB, da Silva AM, Dantas CB, Rodrigues CR, Coutinho SS, Sathler PC, Castro HC, Dias LRS, de Sousa VP, Cabral LM (2011) Preparation and evaluation of a new nano pharmaceutical excipients and drug delivery system based in polyvinylpyrrolidone and silicate. J Pharm Pharma Sci 14(1):17–35
24. Rao YQ, Blanton TN (2008) Polymer nanocomposites with a low thermal expansion coefficient. Macromolecules 41:935–941
25. Wang C, Guan L, Mao Y, Gu Y, Liu J, Fu S, Xu Q (2009) Optical nonlinearity of ZnS–polyvinyl pyrrolidone nanocomposite suspension. J Phys D Appl Phys 42(4):045403–045407
26. Szczerba M, Srodon J, Skiba M, Derkowski A (2010) One-dimensional structure of exfoliated polymer-layered silicate nanocomposites: a polyvinylpyrrolidone (PVP) case study. Appl Clay Sci 47:235–241
27. Wong JY, Bronzino JD (eds) (2007) Biomaterials. CRC Press, Taylor and Francis Group, New York
28. Lindblad M, Liu Y, Albertsson AC, Ranucci E, Karlsson S (2002) Advances in Polymer Science, 157, Degradable Aliphatic Polyesters. Springer-Verlage, Berlin
29. Mallakpour S, Dinari M (2011) Progress in synthetic polymers based on natural amino acids. J Macromol Sci Part A Pure 48:644–679
30. Mallakpour S, Dinari M (2011) Preparation and characterization of new organoclays using natural amino acids and Cloisite Na^{+}. Appl Clay Sci 51:353–359
31. Sinha Ray S, Okamoto M (2003) Polymer/layered silicate nanocomposites: a review from preparation to processing. Prog Polym Sci 28:1539–1641
32. Sinha Ray S, Okamoto K, Okamoto M (2003) Structure–property relationship in biodegradable poly(butylene succinate)/layered silicate nanocomposites. Macromolecules 36:2355–2367
33. Kontou E, Niaounakis M, Georgiopoulos P (2011) Comparative study of PLA nanocomposites reinforced with clay and silica nanofillers and their mixtures. J Appl Polym Sci 122:1519–1529
34. Mallakpour S, Khani M (2015) Spectral, surface and thermal properties of poly(vinylpyrrolidone)/organo-modified-TiO_2/organo-modified-layered silicate ternary nanocomposites containing L-leucine amino acid fabricated by sonication process. J Compos Mater 49:351–361
35. Krevelen DV, Hoftyzer P (1976) Properties of Polymers, 3rd edn. Elsevier, Amsterdam